Magnetic Properties of Surfaces Investigated by Spin-Polarized Electron Beams

D.T. Pierce

National Bureau of Standards, Gaithersburg, MD 20899, USA

A spin-polarized electron beam incident on a ferromagnetic surface results in elastically and inelastically scattered electrons and in photons via radiative transitions. The spin-dependent intensities of each of these provide a sensitive measure of surface magnetization. A comparison between low-temperature spin deviations at the surface and in the bulk is given; the variation follows the same power law with temperature but with a larger prefactor for the surface. The connection between surface electronic structure and surface magnetism and the changes in each induced by chemisorption have been studied by spin-polarized inverse photoemission. For oxygen and carbon monoxide on Ni(110), a reduction of the Ni magnetic moment is found, rather than a decrease in exchange coupling and corresponding randomization of the alignment of the moments. Further, in the case of CO, the chemisorption interaction is nonlocal with one CO molecule eliminating on the average the magnetic moment of two Ni atoms.

1. Introduction.

The surface or solid-vacuum interface comprises a low-dimensional system with magnetic properties which may be different from the bulk of a material for a number of reasons. At the surface the bulk symmetry is broken. There is a lack of translational periodicity, a different number of neighboring atoms for the surface atoms, and possibly even a different arrangement of these atoms. Because the interface between a magnetic material and a second material has many similarities to the solid-vacuum interface, we expect that our studies of the latter will also be important in understanding atomically engineered epitaxial magnetic films, magnetic interfaces, and compositionally modulated (artificially layered) magnetic structures.

There are many questions about the magnetic properties at a surface which one would like to answer.

(1) Structure: What is the spatial variation of the magnetization from the surface into the bulk? Is there a layer-dependent magnetic moment? What is the magnetization variation parallel to the surface, i.e. the domain microstructure?

(2) Magnetization curves: Is the hysteresis loop at the surface different from the bulk? What does this tell us about the role of the surface in domain nucleation or magnetization rotation?

(3) Temperature effects: How do the low-temperature spin deviations at the surface differ from the bulk? How does the magnetization vary with temperature near the Curie temperature? What is the critical exponent? What is the extent of short range magnetic order above the Curie temperature?

(4) Electronic structure: How do the spin-split energy bands vary throughout the Brillouin zone? How are the core levels affected by exchange interactions with magnetic valence electrons?

(5) Chemistry: What magnetic and electronic properties change when a gas overlayer is adsorbed on the surface or when a species is segregated to the surface? What is the connection between changes in the magnetization and changes in the electronic structure?

(6) Excitations: What is the spin-wave dispersion at the surface? What is the spectrum of Stoner excitations?

Electron spectroscopies are widely used in surface studies because low-energy electrons are strongly interacting and have a short inelastic mean free path in the material. In contrast to bulk probes such as conventional neutron or x-ray measurements, optical techniques, or transmission electron microscopy, low-energy electrons probe only the outer few atomic layers. Since some surface disturbances "heal" within an electron probing depth, it is also possible to obtain information on bulk properties. Distinguishing surface and bulk effects is not always straightforward, and caution is necessary in interpreting the data. In certain instances, such as the addition of an overlayer, the effect of the perturbation is localized at the surface and the induced changes are readily observed.

Normally, electron spectroscopies measure electronic properties and are insensitive to magnetic properties. However, when the spin polarization of the electrons is added as a parameter in studies of systems with a net spin orientation, such as ferrimagnets or ferromagnets, information can be obtained about the size of the magnetic moment as well as the degree of magnetic order. The component along the z direction of the spin polarization vector $\vec{P}$ of an electron beam is defined as

$$P_z = \frac{n_+ - n_+}{n_+ + n_+} , \qquad (1)$$

where n_+ and n_+ are respectively the number of electrons with electron-spin parallel or antiparallel to the z direction. In studies of magnetic surfaces, the preferred direction is given by the magnetization or by the orientation of the net spin density of the material.

The answers to our questions about the magnetic properties of surfaces are accessible using a variety of experimental techniques involving spin-polarized electrons. The techniques can be conveniently divided into three categories: (a) polarized electrons in and photon or electron intensities out, (b) photons or unpolarized electrons in and polarized electrons out, and (c) polarized electrons in and polarized electrons out.

In the first category are spin-polarized electron scattering and polarized low-energy electron diffraction (PLEED). These techniques have been used to investigate surface magnetization (hysteresis) curves [1] as well as low temperature spin deviations [2] (see Section 2) and critical behavior [3]. In principle it is possible to use PLEED to extract layer-dependent magnetization if measurements are made at sufficiently low temperature; analysis [4] of higher temperature data is difficult owing to thermal fluctuations of the spin orientations which tend to be comparable to or larger than the intrinsic variation to be determined. In addition to these elastic scattering examples, inelastic polarized electron scattering has been used to detect Stoner excitations [5]. Another example which can be considered a type of inelastic scattering is spin-polarized inverse photoemission (Section 3). In this technique polarized incident electrons lose energy through excitation of radiative transitions in the target, and the resulting photons are detected. Such measurements have been used to investigate spin dependent electronic structure [6,7]. They have been especially fruitful in studying the connection between chemisorption-induced changes in surface magnetism and electronic structure [8-10].

Experimental techniques in the second category (b) involve the measurement of the spin polarization of an electron beam. Spin-polarized photoemission is the oldest [11] such technique and has been used with great success to study spin-dependent electronic structure [12,13], effects of chemisorption [14], and even short-range magnetic order near the Curie temperature [15]. The first measurement of the energy spectrum [16] of the spin polarization of low-energy secondary electrons emitted from a ferromagnetic material showed an enhancement of the

polarization at low energies which was subsequently observed on other materials [17-19] and discussed theoretically [20,21]. Some depth resolution is possible by varying the secondary emission parameters. This makes it possible to compare surface and bulk hysteresis curves [22]. When the secondary electrons are excited by a finely focused electron beam in a scanning electron microscope, the magnetic domain microstructure can be imaged [23,24]. Spin-polarized Auger spectroscopy, the newest of these techniques in category (b), provides information on spin-dependent electronic structure and surface chemistry, and has the advantage that element specific magnetic information can be obtained [25]. Further examples of fruitful applications of polarized electron spectroscopies can be found in a number of reviews [12,26,27].

The third category (c) of experiments, in which the incident electrons are spin polarized and spin analysis takes place after the interaction, combines the difficulty of the previous two categories. One experiment of this type has been reported in which Stoner excitations in iron are investigated by using low-energy inelastic scattering of a polarized electron beam with measurement of the polarization of the scattered electrons [28]. With sufficient energy resolution, such experiments will also be able to map surface magnon dispersion curves.

Many of the examples cited above take advantage of the possibility of also using electrons to investigate bulk properties. In this chapter we are concerned with magnetic properties of low-dimensional systems and will focus on some experimental results on the magnetic properties of surfaces using two techniques of category (a). In Section 2 we discuss spin-polarized elastic scattering studies of low-temperature surface spin deviations. In Section 3 we use spin-polarized inverse photoemission to determine the connection between surface magnetism and electronic structure and the changes induced by chemisorption of overlayers of oxygen and carbon monoxide on a Ni(110) surface.

2. Spin Polarized Electron Scattering.

A. Spin Dependent Interactions.

When a spin-polarized electron beam is scattered from the surface of a material, the scattered intensity may depend on the orientation of the spins of the incident electrons. The important terms of the interaction Hamiltonian can be written

$$H = \Sigma_i V(\vec{r}-\vec{r}_i) + \Sigma_i \frac{1}{2m^2c^2}\frac{1}{|\vec{r}-\vec{r}_i|}\frac{dV(\vec{r}-\vec{r}_i)}{dr}\vec{s}\cdot\vec{L} + \Sigma_i J(\vec{r}-\vec{r}_i)\,\vec{s}\cdot\vec{S}_i \quad , \quad (2)$$

where $\vec{r}$ is the position of the incident electron with spin $\vec{s}$ and angular momentum $\vec{L}$, $\vec{r}_i$ is the position of the i-th atom with spin $\vec{S}_i$, and $J(\vec{r}-\vec{r}_i)$ is the exchange integral. The first term is the spin-independent scattering potential, the second is the spin-orbit scattering potential, and the third is the spin-dependent part of the exchange potential. The last term can be written in terms of the net spin density, i.e. $\vec{S}_i$ need not be a localized atomic spin; the spin dependent part of the exchange-correlation potential of VON BARTH and HEDIN [29] can be cast in this form [30].

By reversing the orientation of the incident electron spin $\vec{s}$ it is possible to isolate the spin-dependent scattering from the spin-independent part arising from the first term of (2). Further, if $\vec{s}$ lies in the scattering plane and therefore perpendicular to $\vec{L}$, one discriminates against the spin-orbit scattering. Alternatively, by reversing the magnetization and hence the direction $\vec{S}_i$ of the net spin density of the target, the spin dependence of the scattering that arises solely from the target surface magnetization can be isolated. As can be seen from (2), if there is a decrease in the magnetization either by the spins $\vec{S}_i$ becoming disordered or if the magnetic moment per atom (i.e. $\vec{S}_i$) decreases, it will be observed by the electron scattering.

We define a scattering asymmetry

$$A = \frac{I_+ - I_+}{I_+ + I_+} \quad , \quad (3)$$

where I_+ and I_+ correspond to the intensity of the scattered electrons when the incident electron beam is 100% spin polarized parallel and antiparallel, respectively, to the net spin density of the sample. For single scattering within the first Born approximation, it can be shown that the asymmetry is directly proportional to the magnetization [31,32],

$$A(\vec{K}) \propto \frac{J(\vec{K})}{V(\vec{K})}\frac{M(T)}{M(0)} \quad , \quad (4)$$

where $\vec{K}$ is the momentum transfer and $J(\vec{K})$ and $V(\vec{K})$ are the Fourier transforms of the exchange and Coulomb potentials. While A is frequently proportional to the magnetization, this is not true in general when multiple scattering is present [13]. Then we have

$$A = \alpha M(T) + \beta M(T)^3 + \gamma M(T)^5 + \ldots \quad (5)$$

and special care must be taken in interpreting the scattering data.

B. The Spin Polarized Electron Source.

The key to spin-polarized electron scattering experiments, or the inverse-photoemission experiments of Section 3, is having an electron gun which produces spin-polarized electrons with a direction of polarization that can be easily reversed. Such a source of spin-polarized electrons is realized in an electron gun which uses negative electron affinity (NEA) GaAs as a photocathode [34]. The polarization of the electrons results from selection rules governing the photoexcitation of electrons with circularly polarized light from the spin-orbit-split valence band to the conduction band of GaAs. The theoretical spin polarization changes from +50% to -50% when the helicity of the light is reversed.

In addition to producing spin-polarized electrons, the GaAs photocathode, when treated with cesium and oxygen to obtain a negative electron affinity, is a very efficient photoemitter. Therefore, with lasers of only moderate power, it is possible to obtain very intense electron beams. In short, the NEA GaAs polarized-electron gun achieves the favorable characteristics of a conventional electron gun. Additionally it yields a spin-polarized electron beam in which the spin polarization is easily modulated. The time structure of the electron beam intensity is also easily controlled by controlling the time structure of the exciting laser radiation. The energy spread of the beam varies from about 200 meV, for a cathode activated for optimum intensity, down to a remarkable 30 meV for a cathode activated for minimum energy spread [35]. While crucial to the measurements we describe, the operating principles and characteristics of the spin-polarized electron gun have been described [34] in great detail elsewhere and will not be further discussed here.

C. Low Temperature Spin Deviations.

Deviations at finite temperature from the perfect alignment of the electron spins at 0 K are known to occur by thermal excitation of spin waves or magnons. The ratio of the bulk magnetization at a temperature T, $M_b(T)$, to the bulk magnetization at zero temperature $M_b(0)$, follows the Bloch law

$$M_b(T)/M_b(0) = 1 - B_b T^{3/2} + \ldots \quad . \quad (6)$$

The constant B_b is characteristic of long-wavelength spin waves. The next higher

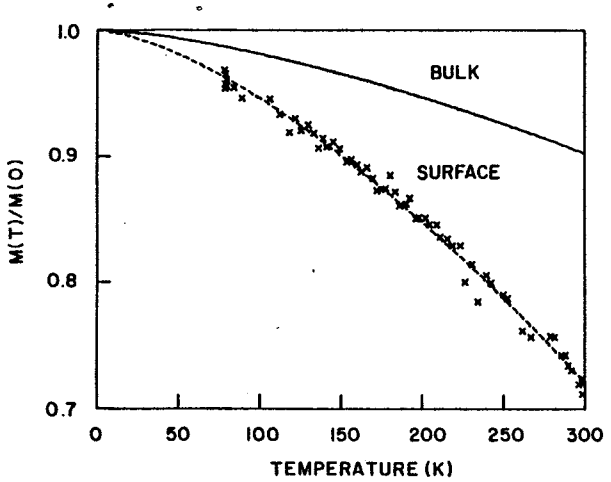

Figure 1. The temperature dependence of the surface magnetization (points) measured by polarized electron scattering is compared to that of the bulk (solid line) determined by conventional methods

order term, proportional to $T^{5/2}$, has been found to be small for amorphous ferromagnets at temperatures less than half the Curie temperature, T_c [36].

At the surface, the boundary conditions are different, and the deviation of the spontaneous magnetization from its zero-temperature value can be different from that in the bulk. Assuming that standing spin waves have antinodes at the surface, RADO [37] predicted in 1957 that the surface magnetization would decrease as $T^{3/2}$ but with a coefficient B_s twice the bulk value B_b. In a more extensive calculation, including both surface and bulk spin waves, MILLS and MARADUDIN [38,39] found that the surface spin-wave contribution is exactly cancelled by a reduction in the bulk spin-wave contribution, again leading to a $T^{3/2}$ temperature dependence with B_s twice the value of B_b. Although this result was obtained within the Heisenberg model, it is also expected to hold for itinerant systems at low temperatures where the spin waves have long wavelengths. These predictions of surface magnetic behavior remained untested for many years. The availability of a spin-polarized electron gun allowed the exploitation of the magnetic and surface sensitivity of polarized electron scattering to make such a test. Results are shown in Figure 1 for scattering from a ferromagnetic glass $Ni_{0.40}Fe_{0.40}B_{0.20}$ at an energy E = 90 eV and a scattering angle θ = 166°. The applied field (remanent field of C-shaped electromagnet) was maintained at a constant value such that the sample was a single domain. The measured temperature dependence of the scattering asymmetry A(T) was shown to be proportional to the magnetization of the ferromagnetic glass [2]. The observed $T^{3/2}$ behavior represented by the dashed-line least-squares fit to the data from 80 K to 300 K was extrapolated to 0 K to compare with the relative bulk magnetization which was measured independently. If we plot the relative surface magnetization vs. the relative bulk magnetization at each temperature as in Figure 2, a straight line is obtained indicating that they both obey the same power law. The slope of the line, which is B_s/B_b, was found to be -3. This value is a lower limit since the average electron probing depth was about 1.5 layers and some subsurface region was sampled.

The discrepancy between the experimental result and the theoretical prediction is attributed to the simplifications of the theory rather than a fundamental fault. The theory is for a simple cubic Heisenberg ferromagnet with uniform magnetic moments and exchange coupling. Extending the theory to allow, for example, for a reduced exchange coupling between the surface layer and the bulk compared to the bulk-bulk exchange coupling would lead to a larger B_s/B_b.

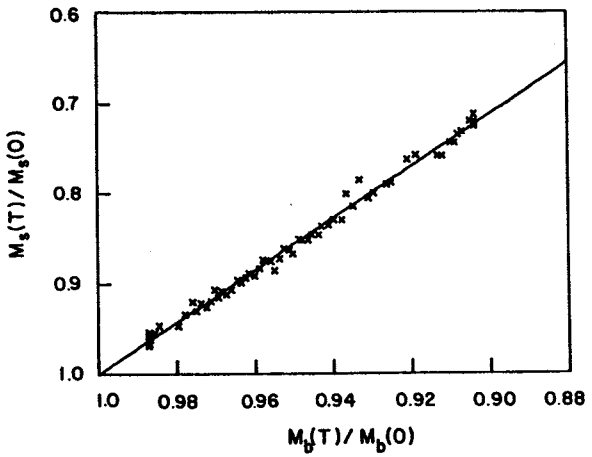

Figure 2. $M_s(T)/M_s(0)$ and $M_b(T)/M_b(0)$ have a linear relationship indicating that they vary with temperature according to the same power law. The slope of the line in B_s/B_b - 3.

3. Spin Polarized Inverse Photoemission.

A. The Technique.

In an ultraviolet photoemission experiment, a photon of known energy excites an electron from a filled state to an unfilled state above the vacuum level where it escapes into the vacuum. By measuring the kinetic energy of the electron, one then also knows the initial-state energy within the uncertainty of relaxation and screening effects. From the angle of emission, the parallel component of momentum k_{par}, which is conserved in the process, is also determined. Photoemission has in this way been able to map energy bands of materials and provide great insight into electronic properties [40].

In the approximately inverse process, a collimated electron beam is incident at a known energy and well defined angle (i.e. specific k_{par}) on the sample. If the electrons are of sufficiently low energy, any radiative transitions which occur will produce ultraviolet photons with negligible momentum. In this inverse photoemission process (also known as ultraviolet bremsstrahlung isochromat spectroscopy), the direct (vertical) transitions between bands allow one to map the energy bands of the unfilled states [41,42].

Shortly after the first k-resolved inverse photoemission measurements were demonstrated [43,44], it was possible, by replacing the conventional electron gun with a spin-polarized electron gun, to demonstrate [6] spin-polarized inverse photoemission spectroscopy (SPIPES). If the incident beam is spin polarized, the electron couples into an initial state of that particular spin orientation from which it can decay radiatively via a direct transition into an empty final state of the same spin. Thus it is possible to determine the spin-dependent band structure of a ferromagnetic material. In particular, in contrast to photoemission, with inverse photoemission it is possible to probe the energy range between the Fermi level and the vacuum level. Exchange-split unfilled d and f levels, which are important for ferromagnetism of materials, lie in this energy range.

The experimental apparatus is similar to that for electron scattering but instead of a Faraday cup to detect the electrons, a Geiger-Mueller counter detects

the photons. The Geiger-Mueller counter [45] has a peak sensitivity at 9.7 eV and band pass of 0.7 eV determined by the combined effects of the iodine photoionization threshold and the ultraviolet transmission cutoff of the CaF_2 window. Advantages of such a detector are its simplicity and large solid angle of photons accepted. Spectra were obtained by varying the incident-electron energy and measuring at fixed photon energy. Although all SPIPES measurements to date have been made in this mode, spectrometers to select the photon energy will be used in the future.

B. A Ferromagnetic Surface: Ni(110).

The capability of SPIPES to investigate the electronic structure in the energy range between the Fermi energy and the vacuum level is used to advantage in studying the Ni(110) surface. A rather flat minority-spin d band of Σ_2 symmetry protrudes above the Fermi level as seen in the energy band diagram [6] of Figure 3. It is such minority-spin d holes that give rise to the average magnetic moment per atom in Ni of approximately a half Bohr magneton. Transitions to this d hole band can be detected very clearly as illustrated in the spectrum [46] of Figure 4. The spin-integrated (dashed curve) at an angle of incidence of 5° shows two peaks, but in the spin-resolved spectra at the bottom of the figure one observes three peaks, if the spin-split peak is counted as one. Transitions of the type A in Figure 3 give rise to the peak (1) in the minority spectrum. Exactly at normal incidence this transition is symmetry forbidden and grows in intensity at increasing angles of incidence.

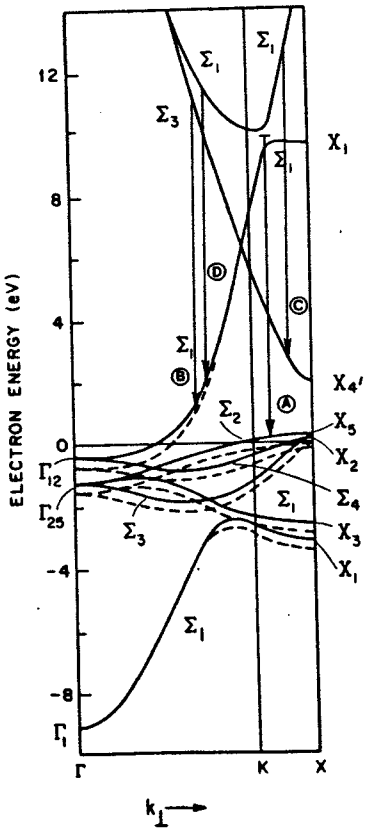

Figure 3. Band structure of Ni along the ΓKX direction showing energetically possible radiative transitions at $\hbar\omega = 9.7$ eV for electrons incident normally on the Ni(110) surface. Dashed curves distinguish the majority spin d bands.

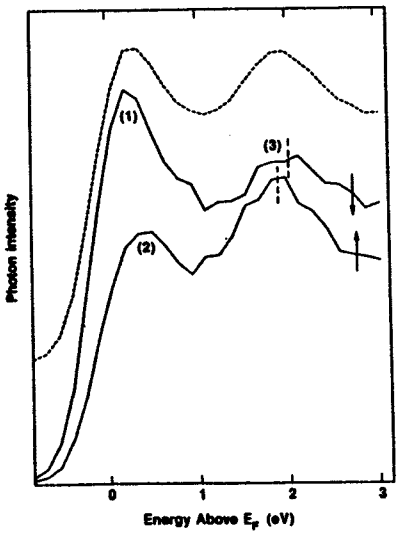

Figure 4. K-resolved spin-polarized (solid curves) and spin-integrated (dashed curve shifted upward) inverse photoemission spectra of Ni(110) are compared at an angle of incidence of 5°. The photon intensity is shown as a function of the final-state energy of the electron with respect to the Fermi level.

The origin of peak (2) in Figure 4 is different [46] from peak (1) as was seen from (i) its different energy position, (ii) its different dispersion and intensity variation with changing k_{par}, and (iii) its different behavior with oxygen chemisorption. It is not a majority spin replica of peak (1) such as would be observed if the sample were incompletely magnetized. Rather, peak (2) was attributed to the transitions of type (B) in Figure 3; the minority counterpart to peak (2) is obscured by peak (1) in the minority-spin spectrum.

The peak at -2 eV above E_F is spin split. Further investigation of this peak showed that the splitting vanished when the sample was demagnetized, confirming its magnetic origin. This peak corresponds to a transition of type C in Figure 3. The splitting is not attributed to an exchange splitting of the s,p manifold itself but rather is an indirect consequence (via s-d hybridization) of the exchange splitting of the d band [46]. From second order perturbation theory, the s, p bands are shifted upward by an amount $H_{sd}^2/(E_s - E_d)$ where H_{sd} is the hybridization matrix element and E_s and E_d are the unperturbed band energies. Because of the exchange splitting of the d bands, the perturbation will have two values. This was the first observation of such a "differential" hybridization shift [46].

The energy bands of Figure 3 are calculated for electrons moving in bulk Ni normal to the (110) surface. With the estimated average 3-4 atomic layer probing depth of the SPIPES measurement for this surface, one would expect to see both bulk and surface features. In the absence of pronounced surface states or other perturbations at the surface, one cannot discern specifically surface features in the spectrum of Figure 4, which has a mixed surface and bulk origin. On the other hand, if there is a specific surface disturbance, such as a chemisorbed overlayer, the effect is clearly observed as described in the next section.

C. Chemisorption Induced Changes in Surface Magnetism.

The differences between the magnetic properties of a bulk ferromagnet and those of a low-dimensional system, such as a surface or interface, are intimately connected to differences in electronic structure. Traditionally, the relationship between surface magnetism and chemisorption has been explored using bulk magnetic measurements of high surface area samples [47]. In such measurements the connection to changes in electronic structure are not addressed. As discussed in the previous section, SPIPES allows one to distinguish transitions to particular final states, that is, to determine which electronic state or orbitals are actually involved in the chemisorption induced changes. We will focus on transitions to the minority-spin d hole states which give rise to the magnetic moment, and observe how these states change with chemisorption. Two quite different chemisorption systems, oxygen and carbon monoxide, will be discussed. The oxygen chemisorbs dissociatively, induces a 2x1 reconstruction of the Ni(110) surface, and sits in the long bridge site. Beyond initial rapid chemisorption at coverages of $\theta \lesssim 0.5$ monolayer, there is nucleation and growth of NiO islands which are two to three layers thick [48]. Carbon monoxide, in contrast, chemisorbs molecularly, bonds predominantly in the terminal or on-top position, resides purely on the surface, and induces no reconstruction.

The role of the d electrons in chemisorption bonding is a topic of current discussion and dispute [49,50]. It has been suggested [49] that they are only weakly involved in the bonding, in which case the chemisorption may have only a weak and indirect effect on the surface electronic structure and surface magnetism as manifested by the d-hole spectrum. Alternatively, one might expect that there is a transfer of electrons to the electronegative oxygen which, depending on their relative spin orientation, might increase the surface magnetization. There are two distinct ways the surface magnetism can be decreased. First, without changing the size of the average moment, the chemisorption could cause a reduction of the exchange coupling in the surface resulting in the moments becoming randomly oriented. In this case one would still observe d-holes (i.e., the spin-integrated spectrum would be unchanged). However, there would be no preferred orientation, and a majority peak at the same energy as the minority-spin d-hole peak would be

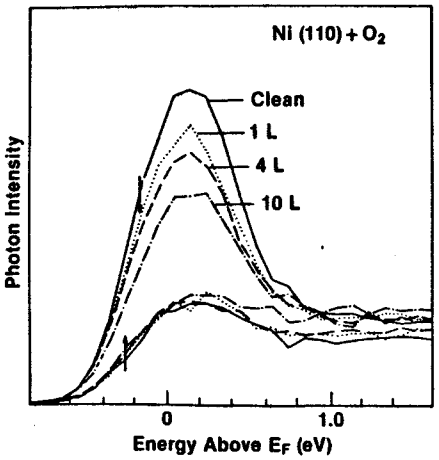

Figure 5. Spin-polarized inverse photoemission spectra, at an angle of incidence of 25°, of clean Ni(110) and after exposure to 1, 4, and 10 L of O_2. At each coverage two photon intensity spectra are shown, one for minority spin (↓) and the other for majority spin (↑) polarization of the incident electron beam.

produced by emission from surface atoms. Alternatively, if the chemisorption by some mechanism caused a reduction in the magnetic moment, i.e. in the number of d holes, one would only expect to see a decrease of the minority-spin peak of the SPIPES spectrum.

The effect of oxygen chemisorption is illustrated [8,9] by the spectra of Figure 5 for exposure of 1, 4, and 10 L (1 L = 10^{-6} Torr-sec) which corresponds to coverages of 0.3, 0.45, and 0.62 monolayer of oxygen. The major change that takes place at exposure up to 10 L is a reduction in the minority-spin d peak. There is no change in the small-majority spin peak which corresponds to transitions to a different final state; this indicates that electron attenuation in the overlayer cannot be an important cause for the decrease of the minority-spin d peak. Equally important as the reduction of the minority- spin peak is the absence of a growth of a corresponding majority-spin peak at the same energy as expected if the chemisorption just affects the exchange coupling and randomizes the moments. Nor is there any appearance of a majority- spin peak as might be expected if the chemisorption caused a decrease in the exchange splitting via a rigid shift of the bands.

These results from oxygen on Ni(110) can be compared to a similar investigation [51] of CO on Ni(110). As in the case of oxygen chemisorption, there is initially a smooth decrease of the minority-spin d peak with no concurrent growth of a majority-spin peak. [Unlike the case of oxygen, there was a slight but reproducible decrease in the majority-spin peak (2), but this change was minor and confined to the first 0.5 L of CO exposure.] Therefore, one knows that large decreases in the leading peak of the spin-integrated spectra result from the decrease in the minority-spin peak. Both the relative intensity of the leading peak in the spin-integrated spectra and the minority-spin spectra are plotted in Figure 6. Spin integrated spectra can be obtained faster with good statistics and for this reason were measured over a higher density of exposures and a wider range of final-state energies.

In contrast to the chemisorption of oxygen on Ni(110) where no oxygen antibonding peak was observed, a CO antibonding peak at 3.7 eV above the Fermi level was observed due to transitions into the CO π^* level. The relative intensity of this CO π^* peak is also shown as a function of coverage in Figure 6. The contribution to the spin-dependent photon asymmetry from transitions into the CO π^* level above the inelastic background was found [51] to be zero, $A = 0 \pm 0.02$.

On comparing the behavior of the Ni minority-spin peak and the CO π^* peak in Figure 6, a major difference is noted. Whereas the CO peak increases uniformly

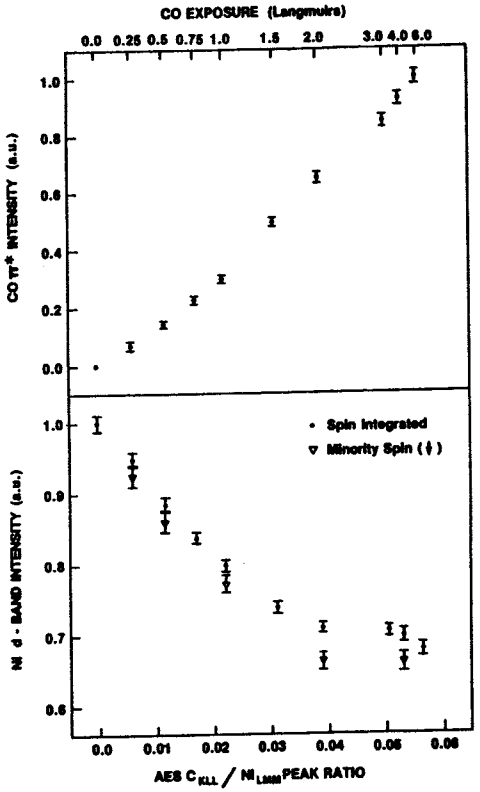

Figure 6. Intensity of spin-integrated inverse photoemission into the Ni d-band and CO π^* band, and spin-resolved inverse photoemission into the minority-spin band plotted as a function of coverage given by the AES C(272 eV)/Ni(848 eV) peak ratio. Error bars represent 2σ uncertainties from pulse counting statistics. Note that the CO intensity increases with coverage, whereas the decrease in the intensity of transitions to the d-band saturate at an AES ratio of ~0.03 which corresponds to 0.5 monolayer coverage.

with coverage, the Ni peak decreases and saturates at the Auger electron spectroscopy peak height ratio of 0.03 which is equivalent to 0.5 monolayer coverage [52]. There is no change in the surface magnetization after one CO molecule is adsorbed for each two Ni surface atoms. This result is in agreement with ferromagnetic resonance measurement of CO adsorption on thin Ni films where Göpel found that one CO effectively eliminated the surface magnetism of two Ni atoms. Such an effect is clearly nonlocal.

The nature of this nonlocal effect is clarified by the SPIPES measurement. As discussed in the case of oxygen, if the effect of chemisorption were to reduce the exchange coupling and randomize the orientation of the (still existing) moments, we would see the growth of a corresponding majority-spin d peak. Rather, the CO reduces the moment not only of the Ni atom involved in the chemisorption bond, but also of the Ni atoms in the vicinity of the CO adsorption site.

For both oxygen and carbon monoxide chemisorption on Ni(110) there is a substantial shifting of the density of states within the d-bands and even redistribution of state density between the d-bands. The SPIPES measurement has shown particular sensitivity to such changes. LIEBSCH [54] calculated for the related system, C(2x2)O/Ni(100), that the interaction of the O $2p_z$ states and the d-bands changed the density of states such that the minority-spin band of Ni(110) may be drawn below the Fermi level. A similar effect was found in calculations [55] of NiCO which show that the CO causes a change from a Ni d^9 to a d^{10} configuration. In another study of a larger cluster [56], Ni_{13} + CO, the unfilled minority-spin band was pushed below the Fermi level by CO chemisorption. The

moments of all 13 Ni atoms in the cluster were changed clearly indicating a nonlocal effect. In other theoretical work [57,58], all-electron local-density functional slab calculations are now becoming available for C(2x2)O/Ni(100) and C(2x2)CO/Ni(100). SPIPES measurements of chemisorption on the Ni(100) surface will be able to test these calculations and some of the interesting predictions, such as a "spin-polarized" oxygen antibonding level on Ni(100) [57].

Acknowledgments.

The contributions to the work described in this chapter by my coworkers at NBS, R. J. Celotta, J. Unguris, C. S. Feigerle, and A. Seiler, and by visiting scientists H. C. Siegmann (ETH-Zurich) and J. L. Peña (Cinvestav-Mexico) are gratefully acknowledged. Thanks are also due to N. V. Smith who provided the Ni band structure and assisted in the analysis of the clean Ni(110) data. This work was supported in part by the Office of Naval Research.

References.

1. J. Unguris, D. T. Pierce, and R. J. Celotta, Phys. Rev. B 29, 881 (1984).
2. D. T. Pierce, R. J. Celotta, J. Unguris, and H. C. Siegmann, Phys. Rev. B 26, 2566 (1982).
3. S. F. Alvarado, M. Campagna, F. Ciccacci, and H. Hopster, J. Appl. Phys. 53, 7920 (1982).
4. R. Feder, S. F. Alvarado, E. Tamura, and E. Kisker, Surf. Sci. 127, 83 (1983).
5. J. Kirschner, D. Rebenstorff, and H. Ibach, Phys. Rev. Lett. 53, 698 (1984).
6. J. Unguris, A. Seiler, R. J. Celotta, D. T. Pierce, P. D. Johnson, and N. V. Smith, Phys. Rev. Lett. 49, 1047 (1982).
7. J. Kirschner, Surf. Sci. 162, 83 (1985).
8. A. Seiler, C. S. Feigerle, J. L. Peña, R. J. Celotta, and D. T. Pierce, J. Appl. Phys. 57, 3638 (1985).
9. C. S. Feigerle, A. Seiler, J. L. Peña, R. J. Celotta, and D. T. Pierce, J. Vac. Sci. Technol. A3, 1487 (1985).
10. D. T. Pierce, A. Seiler, C. S. Feigerle, J. L. Peña, and R. J. Celotta, J. Magn. and Magn. Mat., 54-57, 617 (1986).
11. G. Busch, M. Campagna, P. Cotti, and H. C. Siegmann, Phys. Rev. Lett. 22, 597 (1969).
12. H. C. Siegmann, F. Meier, M. Erbudak, and M. Landolt, Adv. Electron and Electron Phys. 62, 1 (1984).
13. E. Kisker, J. Phys. Chem. 87, 3597 (1983).
14. W. Schmitt, H. Hopster, and G. Güntherodt, Phys. Rev. B 31, 4035 (1985).
15. E. Kisker, K. Schröder, W. Gudat, and M. Campagna, Phys. Rev. B 31, 329 (1983).
16. J. Unguris, D. T. Pierce, A. Galejs, and R. J. Celotta, Phys. Rev. Lett. 49, 72 (1982).
17. E. Kisker, W. Gudat, and K. Schröder, Solid State Comm. 44, 623 (1982).
18. M. Landolt and D. Mauri, Phys. Rev. Lett. 49, 1783 (1982).
19. H. Hopster, R. Raue, E. Kisker, G. Güntherodt, and M. Campagna, Phys. Rev. Lett. 50, 71 (1983).
20. J. Glazer and E. Tosatti, Solid State Comm. 52, 905 (1984).
21. D. R. Penn, S. P. Apell, and S. M. Girvin, Phys. Rev. Lett. 55, 518 (1985).
22. R. Allenspach, M. Taborelli, M. Landolt, and H. C. Siegmann, Phys. Rev. Lett. 56, 953 (1986).
23. K. Koike and K. Hayakawa, Appl. Phys. Lett. 45, 585 (1985).
24. J. Unguris, G. G. Hembree, R. J. Celotta, and D. T. Pierce, J. Microscopy 139, RP1 (1985).
25. M. Landolt, R. Allenspach, and D. Mauri, J. Appl. Phys. 57, 3626 (1985).
26. J. Kirschner, Polarized Electrons at Surfaces (Springer-Verlag, Berlin-Heidelberg-New York-Tokyo, 1985).
27. R. Feder, Polarized Electrons in Surface Physics (World Scientific Publishing Co., Singapore, 1985).
28. J. Kirschner, Phys. Rev. Lett. 55, 972 (1985).
29. U. von Barth and L. Hedin, J. Phys. F 5, 1629 (1972).
30. D. T. Pierce and R. J. Celotta, Adv. Electron and Electron Phys. 56, 219 (1982).

31. X. I. Saldaña and J. S. Helman, Phys. Rev. B 16, 4978 (1977).
32. R. J. Celotta, D. T. Pierce, G.-C. Wang, S. D. Bader, and G. Felcher, Phys. Rev. Lett. 43, 728 (1979).
33. R. Feder and H. Pleyer, Surf. Sci. 117, 285 (1982).
34. D. T. Pierce, R. J. Celotta, G.-C. Wang, W. N. Unertl, A. Galejs, C. E. Kuyatt, and S. R. Mielczarek, Rev. Sci. Instrum. 51, 478 (1980).
35. C. S. Feigerle, D. T. Pierce, A. Seiler, and R. J. Celotta, Appl. Phys. Lett. 44, 866 (1984).
36. S. N. Kaul, Phys. Rev. B 24, 6550 (1981).
37. G. T. Rado, Bull. Am. Phys. Soc. II 2, 127 (1957).
38. D. L. Mills and A. A. Maradudin, J. Phys. Chem. Solids 28, 1855 (1967).
39. D. L. Mills, Comments Solid State Phys. 4, 28 (1971); 4, 95 (1972).
40. F. J. Himpsel, Adv. Phys. 32, 1 (1983).
41. V. Dose, J. Phys. Chem. 88, 1681 (1984).
42. N. V. Smith, Vacuum 33, 803 (1983).
43. D. R. Woodruff and N. V. Smith, Phys. Rev. Lett. 48, 283 (1982).
44. G. Denninger and V. Dose, Phys. Rev. Lett. 48, 279 (1982).
45. G. Denninger, V. Dose, and H. Scheidt, Appl. Phys. 18, 375 (1979).
46. A. Seiler, C. S. Feigerle, R. J. Celotta, D. T. Pierce, and N. V. Smith, private communication and to be published.
47. P. W. Selwood, Chemisorption and Magnetization (Academic, New York, 1975) and references therein.
48. P. H. Holloway, J. Vac. Sci. Technol. 18, 653 (1981).
49. C. F. Melius, Chem. Phys. Lett. 39, 287 (1976).
50. C. M. Varma and A. J. Wilson, Phys. Rev. B 22, 3795 (1980); A. J. Wilson and C. M. Varma, Phys. Rev. B 22, 3805 (1980).
51. C. S. Feigerle, A. Seiler, J. L. Peña, R. J. Celotta, and D. T. Pierce, Phys. Rev Lett. 56, 2207 (1986).
52. B. J. Bandy, M. A. Chesters, P. Hollins, J. Pritchard, and N. Sheppard, J. Mol. Spec. 80, 203 (1982).
53. W. Göpel, Surf. Sci. 85, 400 (1979).
54. A. Liebsch, Phys. Rev. B 17, 1653 (1978).
55. C. M. Kao and R. P. Messmer, Phys. Rev. B 31, 4835 (1985).
56. F. Raatz and D. R. Salahub, Surf. Sci. 146, L609 (1984).
57. S. Chubb and A. J. Freeman, to be published.
58. E. Wimmer, C. L. Fu, and A. J. Freeman, Phys. Rev. Lett. 55, 2618 (1985).